Inorg. Chem. **2008**, *47*, 12004−12009

Experimental and Theoretical Characterization of the Hexaazidophosphate(V) Ion

P. Portius,* P. W. Fowler, H. Adams, and T. Z. Todorova

Department of Chemistry, University of Sheffield, Brook Hill, Sheffield, S3 7HF, United Kingdom

Received August 12, 2008

(PPN)$[P(N_3)_6]$ (**2**) was synthesized by the metathesis of $Na[P(N_3)_6]$ (**1**) and $(PPN)N_3$ ($PPN^+ = \{(Ph_3P)_2N\}^+$), allowing for the isolation and full characterization of a stable hexaazidophosphate(V) salt by ^{31}P and ^{14}N NMR, UV absorption, IR and Raman spectroscopy, elemental and thermal analyses, X-ray diffraction, and Hartree−Fock and density functional theory calculations. The colorless single crystals of **2** are triclinic, space group $P\bar{1}$, $a = 9.6296(9)$, $b = 9.8158(9)$, $c = 10.1414(10)$ Å, $\alpha = 92.635(5)°$, $\beta = 93.437(5)°$, $\gamma = 92.105(4)°$, and $Z = 1$. The $[P(N_3)_6]^-$ ion of **2** is isolated in the solid state and adopts S_6 symmetry both in the crystal and in solution. Thermogravimetric analysis and differential scanning calorimetry measurements reveal a surprising thermal stability of **2** (T_{dec} ca. 200 °C). No friction sensitivity was encountered.

Introduction

Covalent phosphorus−nitrogen molecules are difficult to isolate and handle, owing to their highly endothermic character and very low energy barriers, which often cause uncontrolled explosive decomposition.[1,2] Despite recent success with the shock-sensitive binary cyclic P−N molecule $\{NP(N_3)_2\}_3$,[2,3] the related homoleptic phosphorus azides $P(N_3)_3$ and $P(N_3)_5$ could be neither isolated nor structurally characterized.[4−7] Nevertheless, studies of the preparation of the ionic complex $[P(N_3)_6]^-$[6,8−10] revealed the, albeit challenging, accessibility of related homoleptic phosphorus azides. According to these studies, complete removal of the solvent from an acetonitrile solution of $Na[P(N_3)_6]$ (**1**) results in explosion at ambient temperature,[6,8] and the highly energetic salt $[N_5][P(N_3)_6]$[10,11] is extremely shock-sensitive and explodes upon the slightest warming toward room temperature. The introduction of larger, weakly coordinating $R_4N^+$and Ph_4E^+ counterions, R = CH_3 and C_2H_5,[6] E = P and As,[8] leads to somewhat less-sensitive compounds which, however, still easily and violently explode upon slight warming. These characteristics hamper the isolation and characterization of $[P(N_3)_6]^-$, which is thus far limited to vibrational[6,10] and ^{31}P NMR[9] spectroscopy. The recent rapid progress in the quest for new energetic molecules and ongoing research in the area of homoleptic main group azides prompted the investigation of $[P(N_3)_6]^-$ reported in this paper. The synthesis, isolation, and characterization of the first stable hexaazidophosphate(V) salt was achieved by using the nonelectrophilic and bulky bis(triphenylphosphoranylidene)ammonium cation $\{(Ph_3P)_2N\}^+$ (PPN^+).[12,13]

Results and Discussion

$Na[P(N_3)_6]$ (**1**) selectively forms within 1 h under strict exclusion of air and water in acetonitrile by the addition of a PCl_5 solution to a cold suspension containing sodium azide in a more than 2-fold excess, and subsequent warming up to room temperature. Spectroscopic analysis of the brownish reaction solution, which can be stored indefinitely at −30 °C, shows only one singlet ^{31}P NMR resonance at −178.8

* Author to whom correspondence should be addressed. Fax: (+44)114-22-29385. E-mail: p.portius@sheffield.ac.uk.

(1) Tornieporth-Oetting, I. C.; Klapoetke, T. M. *Angew. Chem., Int. Ed. Engl.* **1995**, *34*, 511–520.
(2) Goebel, M.; Karaghiosoff, K.; Klapoetke, T. M. *Angew. Chem., Int. Ed.* **2006**, *118*, 6183–6186.
(3) Muralidharan, K.; Omotowa, B. A.; Twamley, B.; Piekarski, C.; Shreeve, J. M. *Chem. Commun.* **2005**, 5193–5195.
(4) Buder, W.; Schmidt, A. *Z. Anorg. Allg. Chem.* **1975**, *415*, 263–267.
(5) Zeng, X.; Wang, W.; Liu, F.; Ge, M.; Sun, Z.; Wang, D. *Eur. J. Inorg. Chem.* **2006**, 416–421.
(6) Volgnandt, P.; Schmidt, A. *Z. Anorg. Allg. Chem.* **1976**, *425*, 189–192.
(7) Knapp, C.; Passmore, J. *Angew. Chem., Int. Ed.* **2004**, *43*, 4834–4836.
(8) Roesky, H. W. *Angew. Chem., Int. Ed. Engl.* **1967**, *6*, 637.
(9) Dillon, K. B.; Platt, A. W. G.; Waddington, T. C. *J. Chem. Soc. Chem. Comm.* **1979**, 889.
(10) Haiges, R.; Schneider, S.; Schroer, T.; Christe, K. O. *Angew. Chem., Int. Ed.* **2004**, *43*, 4919–4924.
(11) Singh, R. P.; Verma, R. D.; Meshri, D. T.; Shreeve, J. M. *Angew. Chem., Int. Ed.* **2006**, *45*, 3584–3601.
(12) Appel, R.; Hauss, A. *Z. Anorg. Allg. Chem.* **1961**, *311*, 290–301.
(13) Ruff, J. K.; Schlientz, W. J. *Inorg. Synth.* **1974**, *15*, 84–90.

10.1021/ic801536z CCC: $40.75
Published on Web 11/13/2008

Scheme 1

$$PCl_5 \xrightarrow[MeCN]{\text{exc. } NaN_3} \underset{(\mathbf{1})}{Na[P(N_3)_6]} \xrightarrow[(PPN)^+ = \{(PPh_3)_2N\}^+]{+\text{ exc. } (PPN)N_3} \underset{(\mathbf{2})}{(PPN)[P(N_3)_6]}$$

ppm and the complete consumption of PCl_5. Furthermore, a very intense infrared absorption appeared in the region of the asymmetric azide stretching vibrations centered at 2116 cm^{-1} next to very weak bands of HN_3 and an unknown decomposition product at 2138 cm^{-1} and 2172 cm^{-1}, respectively. Addition of the solution containing **1** to $(PPN)N_3$ causes precipitation of NaN_3. The resulting $(PPN)[P(N_3)_6]$ salt (**2**; Scheme 1) forms in high yield from the supernatant solution as white crystals, which show neither noticeable signs of decomposition upon several minutes of exposure to the air nor sensitivity toward friction and static electricity. However, solutions of **2** are highly air-sensitive.

Compound **2** is moderately soluble in CH_3CN and very soluble in THF[14] and stable in both solvents under strict exclusion of air at ambient temperature, whereas rapid decomposition occurs in CH_2Cl_2. The very intense band of N_3^- at 1993 or 2005 cm^{-1} is absent from IR spectra recorded in THF and CH_3CN, respectively, indicating that the $[P(N_3)_6]^-$ ion does not dissociate in these solvents.

Compound **2** shows surprising thermal stability, which can be directly compared with those of the related silicon and germanium salts $(PPN)_2[E(N_3)_6]$ (**3**, E = Si; **4**, E = Ge), which differ solely in the anion charge, the nature of the anions' central atom, and the anion/cation ratio. Melting of **2** occurs at 200−202 °C, 10−20 °C below that of **3** (225 °C) and **4** (211 °C). Rapid heating of sealed capillaries containing 1−2 mg of **2** causes detonation at ca. 263 °C. A combined thermogravimetric (TGA) and differential scanning calorimetry (DSC) analysis reveals that melting at an extrapolated onset temperature (T_{on}) of 191 °C, $\Delta H_f = +68$ kJ mol^{-1}, is followed by a two-step decomposition at $T_{on1} = 242$ °C and $T_{on2} = 297$ °C, accompanied by molar enthalpy changes of −946 and −140 kJ mol^{-1}, respectively. These properties indicate **2** as thermally slightly less-stable than the related silicon and germanium salts **3** and **4** (see Table 1) while releasing significantly more energy per mole upon decomposition during the first step. The second decomposition step at $T_{on2} = 300$ °C (TGA) coincides with the onset of decomposition of $(PPN)N_3$. The thermal behavior of the latter was independently determined in a TGA experiment by subjecting a genuine sample of $(PPN)N_3$ to the same conditions ($T_{on} = 304$ °C). Hence, the substantially lower molar enthalpy change of the second step in comparison with **3** and **4** is largely due to the reduced PPN cation content of **2**. Furthermore, the TGA analysis of **2** shows the onset of an extensive 23% mass loss (−192 g mol^{-1}) associated with the first step already at 192 °C, whereas mass loss in **3** is much smaller (6.1%, −82 g mol^{-1}) and sets in at a considerably higher temperature (263 °C).

Mass spectrometry was used to analyze the evolved gas during the thermal decomposition of **2**. At *ca.* 200 °C, the onset of the current of positive ions was observed under electron impact, with the masses $m/z = 199$ (100%) and 115 (92%) being most abundant. An accurate mass measurement allows these masses to be assigned to $[P(N_3)_4]^+$ (199.009927 amu, +3.6 ppm) and $[P(N_3)_2]^+$ (tentatively). Chemical ionization mass spectra (NH_3) show masses at $m/z = 199$ (100%) and 242 (10%), corresponding to $[P(N_3)_4]^+$ and $[P(N_3)_5H]^+$, respectively. Furthermore, prolonged heating at 210 °C *in vacuo* turns **2** into brownish oil, containing some CH_3CN insoluble material. Fourier transform infrared (FTIR) spectra recorded for a CH_3CN solution of the oil revealed a selective growth of the $\nu_{asym}(N_3)$ absorption band of uncoordinated N_3^- at 2005 cm^{-1} at the expense of the band of $[P(N_3)_6]^-$. Thus, it can be concluded that heating causes the dissociation of $[P(N_3)_6]^-$ into N_3^- and $P(N_3)_5$, which partly evaporates *in vacuo* or decomposes under ambient pressure.

Table 1. Results of Thermal Analyses[a]

		fusion	step 1	step 2	method
$(PPN)[P(N_3)_6]$ (**2**)	T_{on}	191	242	297	DSC
	ΔH	+68	−946	−140	
	T_{on}		192	300	TGA
	Δm		23		
$(PPN)_2[Si(N_3)_6]$ (**3**)	T_{on}	204	256	321	DTA
	ΔH		−824	−430	
	T_{on}		263	325	TGA
	Δm		6.1		
$(PPN)_2[Ge(N_3)_6]$ (**4**)	T_{on}	194	256	312	DSC
	ΔH	+64	−705	−482	
$(PPN)N_3$	T_{on}			304	TGA

[a] Extrapolated onset temperature T_{on}/°C, molar enthalpy change ΔH/kJ mol^{-1}, mass loss Δm/%. Data obtained from differential scanning calorimetry (DSC), thermogravimetric analysis (TGA) and differential thermal analysis (DTA) of the salts **2** and $(PPN)N_3$ (this paper), **3**,[15] and **4**.[16]

An understanding of the relative stability of the $[P(N_3)_6]^-$ salts can be approached through semiquantitative estimates of the energetics of the proposed initial dissociation reactions $(PPN)[P(N_3)_6]_{(s)} \rightarrow (PPN)N_{3(s)} + P(N_3)_5$ (i) and $Na[P(N_3)_6]_{(s)} \rightarrow NaN_{3(s)} + P(N_3)_5$ (ii) based on lattice energy.[17] The gain in lattice energy of reaction i is close to zero, whereas reaction ii leads to a net gain of ca. 240 kJ mol^{-1}. This finding indicates $Na[P(N_3)_6]$ to be thermodynamically less stable than $(PPN)[P(N_3)_6]$, irrespective of the unknown state of $P(N_3)_5$. Furthermore, an analogous reaction involving the salts **3** and **4**, $(PPN)_2[E(N_3)_6]_{(s)} \rightarrow (PPN)N_{3(s)} + (PPN)[E(N_3)_5]_{(s)}$ (iii), leads to a net loss of lattice energy of ca. 170 kJ mol^{-1} each, which contributes to the higher stability of the latter salts in comparison to **2** (see the Supporting Information for further details).

Data for the $[P(N_3)_6]^-$ ion obtained from IR, Raman, and ^{31}P NMR spectra of **2** recorded in solution or the solid state are largely consistent with the literature.[6,9,18] The ^{14}N NMR spectrum of **2** shows three singlet resonances at $\delta = -268$, −141, and −170 ppm due to N_α, N_β, and N_γ atoms of magnetically equivalent azido ligands. [The N_β resonance

(14) The related PPN salts $(PPN)_2[E(N_3)_6]$ (E = Si, Ge) are all soluble in CH_2Cl_2 and CH_3CN but insoluble or sparingly soluble in THF.

(15) Filippou, A. C.; Portius, P.; Schnakenburg, G. *J. Am. Chem. Soc.* **2002**, *124*, 12396–12397.
(16) Filippou, A. C.; Portius, P.; Neumann, D. U.; Wehrstedt, K.-D. *Angew. Chem., Int. Ed.* **2000**, *39*, 4333–4336.
(17) Jenkins, H. D. B; Roobottom, H. K.; Passmore, J.; Glasser, L. *Inorg. Chem.* **1999**, *38*, 3609–3620.
(18) In CH_2Cl_2, the anion resonates at −180.0 ppm: Dillon, K. B.; Platt, A. W. G. *J. Chem. Soc., Dalton Trans.* **1983**, 1159–1164.

overlaps with the solvent ^{14}N resonance at −136.6 ppm and was determined by Lorentzian curve fitting. A ^{14}N resonance of the PPN cation could not be found, which is in accord with the absence of the resonance of $(PPN)N_3$ in the same solvent.] These chemical shifts are within the spectral region defined by the related $[As(N_3)_6]^-$ and $[Sb(N_3)_6]^-$ complexes (As: −253, −142, −163;[19] Sb: −287, −141, −185 ppm[20]) and are clearly distinct from those of doubly charged anions $[E(N_3)_6]^{2-}$ (E = Si,[15] Ge,[16] Se,[21] Te:[22] −297 to −289 ppm, N_α; −139 ppm, N_β; −248 to −208 ppm, N_γ). Near-UV spectra recorded on the low-energy side of the PPN absorption peaks in THF and MeCN solution are nearly identical and show two weak, broad, and overlapped bands assignable to $[P(N_3)_6]^-$. Gaussian deconvolution shows these bands to be centered at 34 700 cm^{-1} ($\varepsilon_{max} \sim 700$ L mol^{-1} cm^{-1}, fwhm ~ 3600 cm^{-1}) and 31 400 cm^{-1} ($\varepsilon_{max;} \sim 100$ L mol^{-1} cm^{-1}, fwhm ~ 1900 cm^{-1}). No signs of self-aggregation have been found.

Raman, IR, and ^{14}N NMR data indicate a highly symmetric structure of the $[P(N_3)_6]^-$ ion; however, no unambiguous assignment among candidate D_3, D_{3d}, and S_6 structures can be made relying on these methods alone.

The solid-state structure of **2** was determined by X-ray diffraction of a single crystal, which was obtained by slow cooling of a warm saturated solution in CH_2CN.[23] Compound **2** crystallized in the triclinic crystal system $P\bar{1}$ with one formula unit per unit cell and consists of discrete anions, each of which is surrounded by eight PPN^+ cations (Figure 1). The complex anion has a strict C_i symmetric structure in which a central phosphorus atom is bound in an octahedral fashion to the N_α atoms of six surrounding azido ligands, creating an unprecedented nitrogen hexa-coordinated PN_6 framework within the resulting $[P(N_3)_6]^-$ complex (Figure 2). The P−N bonds and the P−N−N and N−N−N angles of the individual azido ligands deviate only marginally from each other (Figure 2 caption), causing a slight distortion to a structure that otherwise would have perfect S_6 point-group symmetry. This structural motive appears in all main group element hexaazides bearing a central atom without a stereochemically active lone pair reported to date (E = As, Sb, Si, Ge, Sn, Pb, Se; for refs, see Table 2).

Structural data on hexa-coordinate phosphorus azides are unavailable. However, a comparison with the pentagonal-

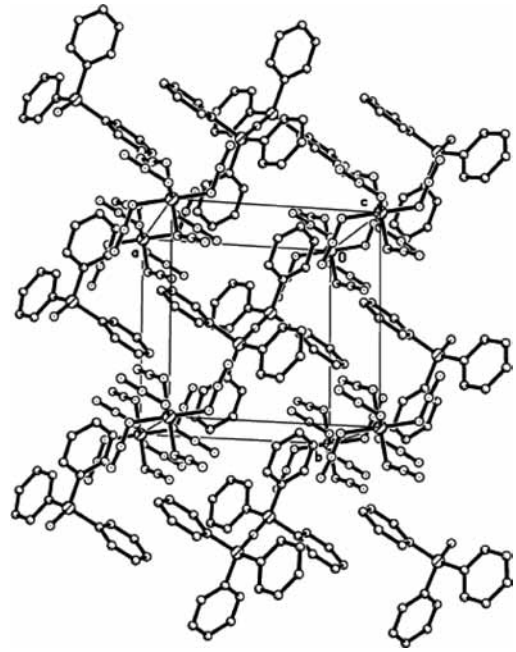

Figure 1. Packing arrangement in the crystal of compound **2** with the vertices of the unit cell occupied by $[P(N_3)_6]^-$ ions, while the center is occupied by the PPN cation; hatched, dotted, and empty circles depict P, N, and C atoms, respectively; H atoms not shown.

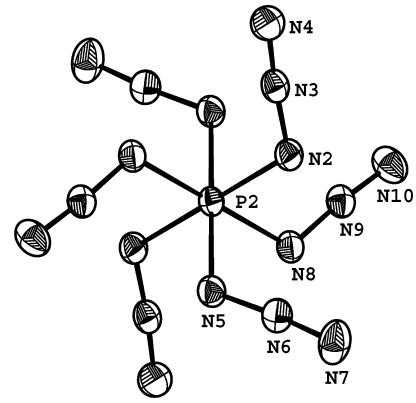

Figure 2. Projection of the $[P(N_3)_6]^-$ anion in **2** down the S_2 axis. The P2 atom is located at a center of inversion. Thermal ellipsoids are set at the 50% probability level. Bond lengths (Å) and angles (deg): P2−N2 1.8121(12), P2−N5 1.8040(12), P2−N8 1.8071(12), N2−N3 1.2290(18), N5−N6 1.2254(17), N8−N9 1.2282(17), N3−N4 1.1325(18), N6−N7 1.1341(18), N9−N10 1.1266(18), P2−N2−N3 117.44(9), P2−N5−N6 118.03(10), P2−N8−N9 117.95(10), N2−N3−N4 175.12(14), N5−N6−N7 175.02(15), N8−N9−N10 174.65(15), N2−P2−N5 89.14(6), N5−P2−N8 91.04(6), N8−P2−N2 89.08(6).

(19) Karaghiosoff, K.; Klapoetke, T. M.; Krumm, B.; Noeth, H.; Schuett, T.; Suter, M. *Inorg. Chem.* **2002**, *41*, 170–179.

(20) Haiges, R.; Boatz, J. A.; Vij, A.; Vij, V.; Gerken, M.; Schneider, S.; Schroer, T.; Yousufuddin, M.; Christe, K. O. *Angew. Chem., Int. Ed.* **2004**, *43*, 6676–6680.

(21) Klapoetke, T. M.; Krumm, B.; Scherr, M.; Haiges, R.; Christe, K. O. *Angew. Chem., Int. Ed.* **2007**, *46*, 8686–8690.

(22) Haiges, R.; Boatz, J. A.; Vij, A.; Gerken, M.; Schneider, S.; Schroer, T.; Christe, K. O. *Angew. Chem., Int. Ed.* **2003**, *42*, 5847–5851.

(23) Crystal data for $C_{36}H_{30}N_{19}P_3$ are as follows: $M = 821.70$; crystallizes from acetonitrile as colorless prisms; crystal dimensions, 0.32 × 0.14 × 0.14 mm^3; triclinic; $a = 9.6296(9)$, $b = 9.8158(9)$, $c = 10.1414(10)$ Å; $\alpha = 92.635(5)°$; $\beta = 93.437(5)°$; $\gamma = 92.105(4)°$; $U = 954.83(16)$ $Å^3$; $Z = 1$; $D_{calcd} = 1.429$ Mg/m^3; space group $P\bar{1}$; C_i^1; No. 2; $\lambda = 0.71073$ Å (Mo Kα); μ (Mo Kα) = 0.213 mm^{-1}; $F(000) = 424$; $T = 150$ K. Data collected were measured on a Bruker Smart CCD area detector with an Oxford Cryosystems low-temperature system. Cell parameters were refined from the setting angles of 7906 reflections (θ range 2.08 < 28.31°). Reflections were measured from a hemisphere of data collected of frames, each covering 0.5° in Ω. Of the 16811 reflections measured, all of which were corrected for Lorentz and polarization effects and for absorption by semi-empirical methods based on symmetry-equivalent and repeated reflections (minimum and maximum transmission coefficients 0.9349 and 0.9708), 4070 independent reflections exceeded the significance level $|F|/\sigma(|F|) > 4.0$. The structure was solved by direct methods and refined by full matrix least-squares methods on F^2. Hydrogen atoms were placed geometrically and refined with a riding model and with U_{iso} constrained to be 1.2 times the U_{eq} of the carrier atom. Refinement converged at a final $R = 0.0385$ ($wR_2 = 0.1082$, for all 4674 data, 265 parameters, mean and maximum δ/σ 0.000, 0.000) with allowance for the thermal anisotropy of all non-hydrogen atoms. Minimum and maximum final electron densities were −0.316 and 0.610 e $Å^{-3}$. A weighting scheme, $w = 1/[\sigma^2(F_o^2) + (0.0675P)^2 + 0.2521P]$ where $P = (F_o^2 + 2F_c^2)/3$ was used in the latter stages of refinement. Complex scattering factors were taken from the program package SHELXTL (an integrated system for solving and refining crystal structures from diffraction data (revision 5.1), Bruker AXS LTD) as implemented on a Viglen Pentium computer.

Table 2. Selected Average Bond Lengths and Angles of the $[E(N_3)_6]^{n-}$ Complexes of Group 14, 15, and 16 Elements[a]

		bond lengths [Å][b]			bond angles [deg][b]	
	$E-N_\alpha$	$N_\alpha-N_\beta$	$N_\beta-N_\gamma$	ΔNN[c]	$E-N_\alpha-N_\beta$	$N_\alpha-N_\beta-N_\gamma$
$(PPN)[P(N_3)_6]$ (**2**)	1.81	1.23	1.13	0.10	118	175
$(py\text{-}H)[As(N_3)_6]$ (**9**)	1.94	1.23	1.13	0.10	116	175
$(Ph_4P)[Sb(N_3)_6]$ (**10**)	2.08	1.22	1.13	0.10	117	175
$(PPN)_2[Si(N_3)_6]$ (**3**)	1.87	1.20	1.15	0.06	124	176
$(PPN)_2[Ge(N_3)_6]$ (**4**)	1.97	1.21	1.15	0.07	120	176
$(Ph_4P)_2[Se(N_3)_6]$ (**11**)	2.13	1.20	1.14	0.07	115	176

[a] E = P, As,[19] Sb,[20] $n = 1$; Si,[15] Ge,[16] Se,[21] $n = 2$. Data were excluded for the ions $[Sn(N_3)_6]^{2-}$,[29] $[Pb(N_3)_6]^{2-}$,[30] and those which possess a stereochemically active lone pair. [b] Rounded mean of the crystallographically independent parameters; uncertainty of the bond lengths is generally smaller than the last digit. [c] $\Delta NN = D_o(N_\alpha-N_\beta) - D_o(N_\beta-N_\gamma)$.

Table 3. Results of HF and DFT Calculations on $[P(N_3)_6]^-$[a]

	bond lengths [Å]				bond angles [deg]	
	$P-N_\alpha$	$N_\alpha-N_\beta$	$N_\beta-N_\gamma$	ΔNN	$P-N_\alpha-N_\beta$	$N_\alpha-N_\beta-N_\gamma$
S_6 RHF/6−311G*	1.804	1.208	1.097	0.111	119.4	176.1
S_6 B3LYP/6−311G*	1.834	1.217	1.137	0.080	120.5	175.1
X-ray [b]	1.808(4)	1.228(2)	1.131(4)	0.097(6)	117.8(3)	174.9(2)

[a] Details of the theoretical calculations are found in the Supporting Information. [b] Unweighted mean x_u of the three crystallographically independent bond lengths and angles of **2** listed.[31]

bipyramidal $PX_4(N_3)$ azido phosphoranes $[P(O-R-O)(O-R'-O)(N_3)]$,[24] $[P(O-R-O)(O-R'-NR'')(N_3)]$,[25] {*cyclo*-$(P(N_3)_3(NPh)\}_2$,[26] and $[P\{N(CH_2CH_2NR)_3\}(N_3)]^+$ (**5**−**8**)[27] and the monoanionic group 15 hexaazides $[As(N_3)_6]^-$ (**9**) and $[Sb(N_3)_6]^-$ (**10**) offers intriguing insight. For instance, the bond lengths and angles of the axial azido group of complexes **5**−**8** adopt values within narrow ranges and fully encompass those of $[P(N_3)_6]^-$, with the exception of slightly longer $P-N_\alpha$ bonds (1.8040(12)−1.8121(12) Å) in the latter. Thus, the overall negative charge and increased coordination number of **2** lengthen the coordinative $P-N_\alpha$ bonds by 3−4 pm with respect to the unstrained phosphoranes **5** and **6**. Furthermore, a close relationship with the hexaazides **9** and **10** can be established on the basis of the range of average $N_\alpha-N_\beta$ and $N_\beta-N_\gamma$ bond lengths, resulting in similar ΔNN bond length differences of ca. 10 pm, as in **2** (Table 2). The doubly charged group 14 and 16 hexaazido anions **3**, **4**, and $[Se(N_3)_6]^{2-}$ (**11**), however, on average exhibit slightly shorter $N_\alpha-N_\beta$ bonds and slightly longer $N_\beta-N_\gamma$ bonds, resulting in smaller ΔNN values (6−7 pm). A comparison of the ΔNN parameter as an indicator for π delocalization along the azido ligand and $E-N_3$ bond ionicity suggests that the ionic character of the coordinative bonds in $[P(N_3)_6]^-$ is similar to that in the As and Sb congeners **9** and **10** but weaker than those of the dianionic complexes **3**, **4**, and **11**. The fact that, unlike $[Si(N_3)_6]^{2-}$ and $[Ge(N_3)_6]^{2-}$, $[P(N_3)_6]^-$ does not react with 2,2′-bipyridine under identical conditions at ambient temperature in acetonitrile solution supports this interpretation.

The results of the X-ray investigation of the structure of the $[P(N_3)_6]^-$ ion are in contradiction with the previously proposed[6] D_{3d} point-group symmetry for the ion in solution. To shed further light on the $[P(N_3)_6]^-$ structure in solution, *ab initio* calculations were carried out.[28] Assignment of idealized S_6 point-group symmetry to the $[P(N_3)_6]^-$ ion was found to be consistent with the results of calculations for the "free" ion. Unconstrained optimization at both RHF/6-311G* and B3LYP/6-311G* levels gave a minimum for a structure of S_6 symmetry, which was checked by an evaluation of the Hessian (energy, geometry, and vibrational frequencies are given in the Supporting Information). The flexibility of this structure is indicated by the presence of angular-distortion modes with extremely low frequencies, the lowest of which was found at 53 cm^{-1} (RHF) and 38 cm^{-1} (B3LYP), respectively. The calculated structural parameters are close to those obtained from X-ray diffraction (see Table 3).

Furthermore, the near neighborhood of the S_6 minimum was explored for other stationary points. Imposition of D_{3d} symmetry yielded only a high-order stationary point on the energy hypersurface, lying 201 and 139 kJ mol^{-1} above the S_6 minimum at RHF and DFT levels, respectively, and six imaginary-frequency modes, $A_{2g} + A_{1u} + E_g + E_u$ at *i*61 to *i*167 cm^{-1} (RHF/6-311G*) and *i*50 to *i*138 cm^{-1} (B3LYP/6-311G*), respectively. Thus, D_{3d} cannot be a candidate for the symmetry of the "free" anion. Relaxation of this structure within the D_3 subgroup of D_{3d} gave a new structure predicted

(24) Kumaraswamy, S.; Muthiah, C.; Swamy, K. C. K. *J. Am. Chem. Soc.* **2000**, *122*, 964–965.
(25) Kumar, N. S.; Kommana, P.; Vittal, J. J. S.; Swamy, K. C. K. *J. Org. Chem.* **2002**, *67*, 6653–6658.
(26) Aubauer, C.; Klapoetke, T. M.; Noth, H.; Schulz, A.; Suter, M.; Weigand, J. *Chem. Commun.* **2000**, 2491–2492.
(27) Thirupathi, N.; Liu, X.; Verkade, J. G. *Inorg. Chem.* **2003**, *42*, 389–397.
(28) Frisch, M. J.; Trucks, G. W.; Schlegel, H. B.; Scuseria, G. E.; Robb, M. A.; Cheeseman, J. R.; Montgomery, J. A., Jr.; Vreven, T.; Kudin, K. N.; Burant, J. C.; Millam, J. M.; Iyengar, S. S.; Tomasi, J.; Barone, V.; Mennucci, B.; Cossi, M.; Scalmani, G.; Rega, N.; Petersson, G. A.; Nakatsuji, H.; Hada, M.; Ehara, M.; Toyota, K.; Fukuda, R.; Hasegawa, J.; Ishida, M.; Nakajima, T.; Honda, Y.; Kitao, O.; Nakai, H.; Klene, M.; Li, X.; Knox, J. E.; Hratchian, H. P.; Cross, J. B.; Adamo, C.; Jaramillo, J.; Gomperts, R.; Stratmann, R. E.; Yazyev, O.; Austin, A. J.; Cammi, R.; Pomelli, C.; Ochterski, J. W.; Ayala, P. Y.; Morokuma, K.; Voth, G. A.; Salvador, P.; Dannenberg, J. J.; Zakrzewski, V. G.; Dapprich, S.; Daniels, A. D.; Strain, M. C.; Farkas, O.; Malick, D. K.; Rabuck, A. D.; Raghavachari, K.; Foresman, J. B.; Ortiz, J. V.; Cui, Q.; Baboul, A. G.; Clifford, S.; Cioslowski, J.; Stefanov, B. B.; Liu, G.; Liashenko, A.; Piskorz, P.; Komaromi, I.; Martin, R. L.; Fox, D. J.; Keith, T.; Al-Laham, M. A.; Peng, C. Y.; Nanayakkara, A.; Challacombe, M.; Gill, P. M. W.; Johnson, B.; Chen, W.; Wong, M. W.; Gonzales, C.; Pople, J. A. *Gaussian 03*, revision B.01; Gaussian, Inc.: Pittsburgh, PA, 2003.

to be a secondary local minimum (34 kJ mol^{-1} above S_6) at the RHF/6-311G* level, again with ultrasoft vibrational modes ($\geq$ 31 cm^{-1}). However, the B3LYP/6-311G* level of theory predicts the same structure to be a doubly degenerate high-order stationary point (i14 cm^{-1}), rather than a true minimum. Relaxation of the D_{3d} structure within the S_6 subgroup of D_{3d} led back to the previous minimum. Intriguingly, a comparison of the molecular shape of the D_3 and S_6 molecules shows that the S_6 structure has adjacent azide groups in closer vicinity and more efficiently avoiding opposing positive partial charges of N_β atoms of adjacent azide groups. The results of frequency calculations were used to distinguish between the D_3 and the S_6 structures using data from FTIR and Raman spectra. The match of relative intensity and position between predicted and observed bands was found to be imperfect with both structures. However, the D_3 structure gives noticeably poorer agreement, as predicted bands due to Raman active vibrations centered at 530 and 750 cm^{-1} were not observed and the predicted relative intensity of an IR band at 575 cm^{-1} is several orders of magnitude higher than was observed. The combination of experimentally determined solid-state structure and the absence of other minima in ab initio quantum mechanical calculation strongly suggests that $[P(N_3)_6]^-$ has in fact S_6 symmetry in solution at room temperature.

In summary, the structure of the energetic ion $[P(N_3)_6]^-$ has been established beyond reasonable doubt in solution and in the solid state. The introduction of the bulky PPN cation has a stabilizing effect both kinetically (spatial separation and phlegmatization of the energetic ions) and thermodynamically (by reduction of the azide nitrogen content and reducing the net gain of lattice energy in an azide dissociation prior to decomposition into dinitrogen). The P−N bonds in $[P(N_3)_6]^-$ are comparably weak as a result of phosphorus hexacoordination. These factors contribute to the marked stability of salt **2** in comparison to the highly explosive and sensitive phosphorus polyazides $P(N_3)_3$ and $\{NP(N_3)_2\}_3$. The hexaazidophosphate has now found a firm place on the landscape of energetic molecules.

Crystallographic data for the crystal structure reported in this paper have been deposited with the Cambridge Crystallographic Database (CCDC No. 697529). This material can be obtained free of charge at www.ccdc.cam.ac.uk/conts/retrieving.html (or from the CCDC, 12 Union Road, Cambridge CB2 1EZ, U.K.; fax: +44 1223 336033; e-mail: deposit@ccdc.cam.ac.uk).

Experimental Section

PCl_5 (Fluka) was sublimed prior to use. NaN_3 (Acros) was dried at 110 °C overnight under high vacuum conditions. Predried acetonitrile (Grubbs) was stored over CaH_2 and added to reaction vessels by vacuum transfer. Filtration was carried out using a stainless steel cannula fitted with a fiberglass filter (Whatman). $(PPN)N_3$ was prepared by a published procedure.[32] Standard Schlenk and glovebox techniques were employed throughout. NMR spectra were recorded on a Bruker 250 MHz (^{1}H, ^{13}C{^{1}H}, ^{31}P{^{1}H}) or 400 MHz (^{14}N) spectrometer run by TopSpin software. Mass spectra, TGA, and DSC measurements were obtained at the Centre for Chemical Instrumentation and Analytical Services at Sheffield, using a VG AutoSpec spectrometer, a Perkin-Elmer Pyris 1 station (under argon, heating rate 10 °C min^{-1}), and a DSC7. Samples for Raman spectroscopy were sealed in glass capillary tubes and spectra recorded between 3800 and 300 cm^{-1} on a Renishaw Ramascope System 2000 spectrometer equipped with a holographic notch filter and a 785 nm diode laser. Only those bands are quoted which are above 2% of the intensity of the main peak. FTIR spectra were recorded between NaCl windows using a Bruker FTIR spectrometer. The spectra of **2** in Nujol suspension contain a number of very weak bands, which are not quoted.

Caution! *Appropriate safety measures need to be taken in attempts to prepare phosphorus polyazides. Filter residues other than* **2** *should not be allowed to dry in the air or in vacuo and should be discarded into dilute aqueous sodium hydroxide.*

In Situ Generation of Na[P(N$_3$)$_6$] (1). A Schlenk tube was charged with PCl_5 (124 mg, 0.595 mmol), and CH_3CN (ca. 10 mL) was added, resulting in a clear and colorless solution. At −30 °C, the solution of the phosphorus chloride was added dropwise to a second Schlenk tube containing a stirred suspension of 14 equiv of NaN_3 (549 mg, 8.44 mmol) in ca. 15 mL of CH_3CN, immersed in a cold bath. The cold bath was then removed and stirring continued for 1 h, after which a brownish suspension had formed, which was left to settle down. Spectra recorded of the orange supernatant solution revealed the formation of the $[P(N_3)_6]^-$ anion, $\tilde{\nu}$ = 3376vvw, 2561vvw, 2116vs, 1288w, 730w, 543w cm^{-1}. NMR ^{31}P{^{1}H} (CD_3CN/CH_3CN, ppm): δ −178.8 (s, $\Delta\nu_{1/2}$ = 56 Hz). The reaction solution was filtered, and the IR-active part of the pale-rose filter residue (493 mg) was identified by FTIR spectroscopy in a nujol mull as being mainly NaN_3 (3391vw, 3300vvw, 2122vs, 640w cm^{-1}). Under the assumption that all $SiCl_4$ has converted, the concentration of $Na[P(N_3)_6]$ in the filter solution is 2.4 × 10^{-2} mol dm^{-3}.

Preparation of (PPN)[P(N$_3$)$_6$] (2). A Schlenk tube was charged with $(PPN)N_3$ (322 mg, 0.555 mmol) and immersed into a cold bath at −35 °C. A total of 19 mL of the solution of $Na[P(N_3)_6]$ (ca. 0.45 mmol) was added dropwise via a transfer cannula while the reaction mixture was stirred. The cold bath was removed, and after several hours, a colorless suspension had formed. The suspension was filtered, which afforded ca. 29 mg of a white solid (according to FTIR mainly NaN_3) that was discarded. At ambient temperature, the volume of the clear and colorless filter solution was diminished until precipitation commenced. The precipitate was redissolved by gentle warming and the resulting solution kept at −30 °C overnight, which resulted in the formation of large colorless crystals. The supernatant solution, containing the excessive $(PPN)N_3$, was filtered off and discarded and the residue washed with approximately 3 mL of CH_3CN and dried in vacuo. This procedure afforded 279 mg of white, crystalline **2** (0.340 mmol), ca. 76% yield with respect to PCl_5, mp = 200−202 °C (sealed glass capillary). Elem. anal. for $C_{36}H_{30}N_{19}P_3$, 821.67 g mol^{-1}, calcd: C,

(29) Fenske, D.; Doerner, H. D.; Dehnicke, K. *Z. Naturforsch., B: Chem. Sci.* **1983**, *38*, 1301–1303.

(30) Polborn, K.; Leidl, E.; Beck, W. *Z. Naturforsch., B: Chem. Sci.* **1988**, *43*, 1206–1208.

(31) Standard deviation given in parentheses (n = 3). Thermal motion in the crystal may produce an apparent shrinkage of the molecular dimensions and is considered by calculating the instantaneous bond lengths D_i, see *Fundamentals of Crystallography*; Giacovacco, C., Ed.; IUCr, Oxford University Press: New York, 1992, resulting in almost no change for the P−N$_\alpha$ and N$_\alpha$−N$_\beta$, distances, whereas N$_\beta$−N$_\gamma$ is affected (D_i ca. 1.140(2) Å).

(32) Martinsen, A.; Songstad, J. *Acta Chem. Scand., Ser. A* **1977**, *31*, 645–650.

52.62; H, 3.68; N, 32.39%; found: C, 52.67; H, 3.48; N, 32.42%. IR (cm^{-1}) $\bar{\nu}$ = 2113 (nujol), 2116 (MeCN), 2115 (CH_2Cl_2), 2112 (THF). Details of IR; Raman; and ^{1}H, ^{13}C, ^{31}P, and ^{14}N NMR spectra can be found in the Supporting Information.

Acknowledgment. We thank the EPSRC (RA114873) for funding and Dr. R. Devonshire and Dr. V. Ramos for recording Raman spectra.

Supporting Information Available: Spectroscopic data of **2**, crystal data and structure refinement, projections of the crystal structure, details of the density functional theory and Hartree−Fock calculations including results of frequency calculations of the S_6 and D_3 minimum structures, IR and Raman intensities and activities, TG and DSC graphs, UV absorption spectra of **2** and $(PPN)N_3$, and empirical lattice energy calculations. This material is available free of charge via the Internet at http://pubs.acs.org.

IC801536Z